

Long-term plasticity of excitatory inputs to granule cells in the rat olfactory bulb

Yuan Gao & Ben W Strowbridge

Using two-photon-guided focal stimulation, we found spike timing-dependent plasticity of proximal excitatory inputs to olfactory bulb granule cells that originated, in part, from cortical feedback projections. The protocol that potentiated proximal inputs depressed distal, dendrodendritic inputs to granule cells. Granule cell excitatory postsynaptic potentials and mitral cell inhibition were also potentiated by theta-burst stimulation. Plasticity of cortical feedback inputs to interneurons provides a mechanism for encoding information by modulating bulbar inhibition.

Long-term behavioral plasticity in the olfactory system has been well established through extensive studies of pheromonal learning^{1,2}, familial recognition in sheep^{3,4} and olfactory conditioning in rodents⁵. However, little is known about the cellular mechanisms that are responsible for olfactory learning. No previous study has demonstrated long-term potentiation (LTP) in the main olfactory bulb using intracellular recordings, although one group recently reported LTP of field potentials evoked by tetanic stimulation in carp⁶. Indirect evidence suggests that one locus of olfactory plasticity may be excitatory inputs to GABAergic granule cells, the primary interneuron in the olfactory bulb. Mitral cell discharges diminish after odor conditioning in neonatal rat pups⁵ and as sheep learn to recognize their newborn lambs at the same time as extracellular GABA increases in the olfactory bulb⁴. We used two-photon imaging to stimulate specific excitatory inputs to granule cells and paired these inputs with postsynaptic action potentials. We found Hebbian LTP and spike timing-dependent plasticity (STDP) of excitatory synapses onto the proximal dendrites of granule cells that arise primarily from feedback projections from piriform cortex^{7,8}.

Focal stimulation near visualized proximal granule cell dendrites evoked fast-rising excitatory postsynaptic potentials (EPSPs) that facilitated with paired stimulation (mean paired-pulse ratio (PPR) = 2.21 ± 0.48 , $n = 11$; **Supplementary Fig. 1** and **Supplementary Methods** online), as reported previously⁸. Pairing synaptic stimulation 10 ms before postsynaptic spikes (+10 ms: 50 shocks at 20 Hz; **Fig. 1a**) triggered a twofold increase in EPSP slope measured 5–15 min after pairing (slope ratio, 2.09 ± 0.32 ; range, 0.88–3.95, significantly greater than 1 ($P < 0.005$), $n = 11$; **Fig. 1b**). Granule cell LTP was robust when analyzed in individual cells. EPSP slope increased in 10 out of 11 granule cells that were tested with one +10-ms pairing protocol; this

increase was statistically significant in 8 of 10 cells that were analyzed individually ($P < 0.05$). EPSP slope typically remained potentiated for the duration of the recording (mean of 25.6 ± 1.5 min after induction); EPSP slope decayed after ~20 min in one granule cell. This form of LTP was not associated with substantial changes in input resistance ($6.90 \pm 1.2\%$ difference; **Fig. 1b**) or holding current (-0.84 ± 1.6 pA change) being required to maintain a constant (-55 mV) membrane potential. The same pairing protocol also potentiated EPSPs that were recorded at -70 mV (**Supplementary Fig. 2** online). Neither repetitive postsynaptic spiking nor extracellular stimulation alone potentiated proximal synapses (slope ratios of 0.91 ± 0.16 and 0.81 ± 0.16 , respectively, $n = 6$, $P > 0.05$; **Supplementary Fig. 3** online). The NMDA receptor antagonist (25 μ M D(-)-2-amino-5-phosphonovaleric acid) prevented proximal EPSP potentiation (slope ratio was 0.67 ± 0.17 , which was significantly different from control ($P < 0.005$), but not significantly different from 1 ($P > 0.05$), $n = 8$; **Supplementary Fig. 4** online), indicating that NMDA receptors are required for LTP at proximal synapses.

Reversing the pairing protocol, evoking postsynaptic spikes 10 ms before stimulating synaptic responses (-10 ms), depressed proximal EPSPs in granule cells (**Fig. 1a**). On average, the EPSP slope ratio was 0.34 ± 0.15 with -10 -ms pairing (significantly less than 1, $P < 0.02$, $n = 4$; **Fig. 1b**). Neither the EPSP PPR nor distance from stimulus position along the apical dendrite was different between the +10 and -10 -ms experiments. The depression of proximal EPSPs evoked by -10 -ms pairing was not associated with a change in input resistance ($6.93 \pm 2.0\%$ difference, $P > 0.05$; **Fig. 1b**) or holding current (-2.1 ± 2.3 pA). Although the +10-ms protocols reliably triggered LTP and the -10 -ms protocols evoked long-term depression, none of the intermediate pairing intervals tested triggered statistically significant plasticity ($P > 0.05$; **Fig. 1c**).

The same +10-ms protocol that effectively potentiated proximal excitatory inputs to granule cells depressed distal, presumed dendrodendritic, inputs that were activated by focal stimulation near visualized distal dendritic segments (slope ratio, 0.59 ± 0.14 , significantly less than 1 ($P < 0.05$), $n = 4$; **Fig. 1d,e**). All distal EPSPs were depressed with paired-pulse stimulation (PPR = 0.73 ± 0.08 , $n = 4$, significantly smaller than the PPR of proximal EPSPs, 2.66 ± 0.25 , $n = 43$, $P < 0.02$; **Supplementary Fig. 1**). These results in the olfactory bulb may be related to the recent finding of bidirectional, location-dependent long-term plasticity in neocortical pyramidal neurons⁹.

We next asked whether tetanic stimulation alone could potentiate excitatory inputs to granule cells. Theta-burst stimulation (TBS, three 50-Hz bursts of five granule cell layer (GCL) shocks, repeated at 5 Hz) increased the number of action currents that were evoked by single test shocks in 7 out of 9 granule cells tested in the cell-attached recording mode (**Fig. 2a**). In all nine cells examined, test stimuli in control conditions appeared to show paired-pulse facilitation, which is typical of proximal synapses onto granule cells, and triggered short-latency

Department of Neurosciences, Case Western Reserve University, Cleveland, Ohio, USA. Correspondence should be addressed to B.W.S. (bens@case.edu).

Received 15 December 2008; accepted 24 March 2009; published online 3 May 2009; doi:10.1038/nn.2319

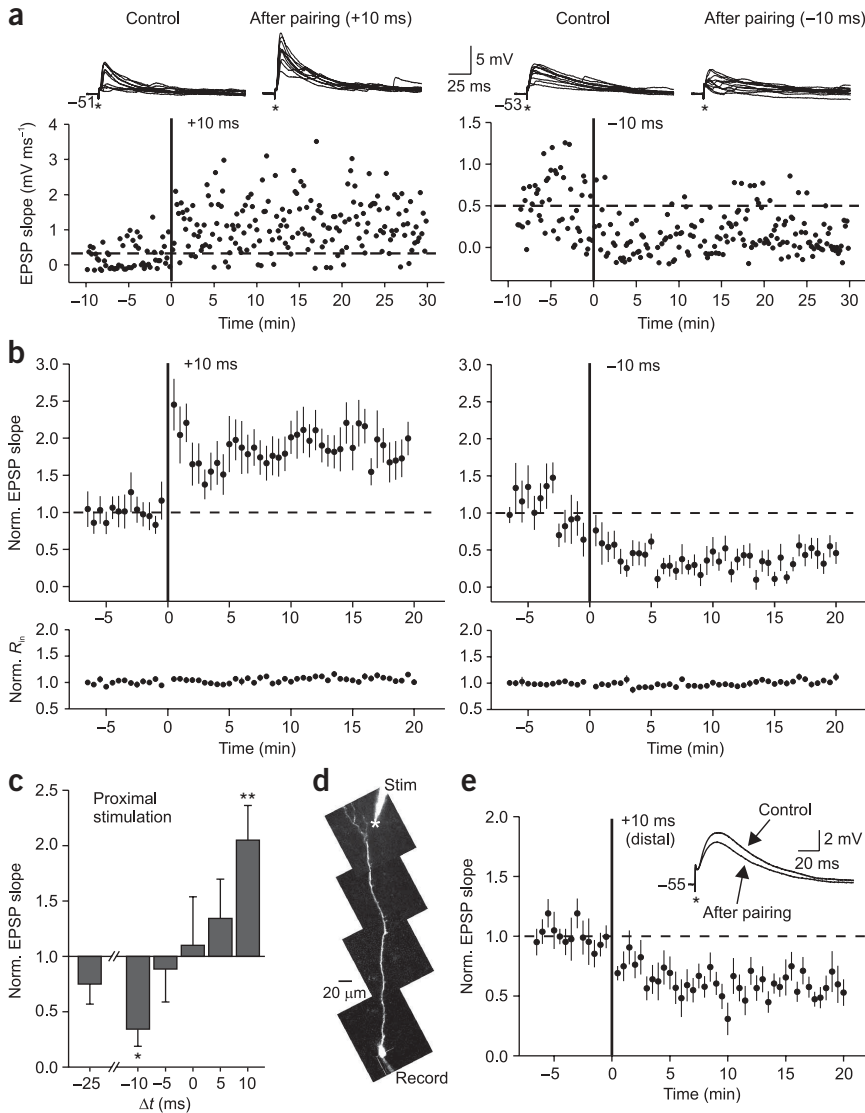


Figure 1 Spike timing-dependent plasticity of proximal excitatory inputs to granule cells. **(a)** Left, potentiation of proximal EPSPs by +10-ms pairings. The time of the pairing is indicated by the vertical line in plot. Example traces from before and 17 min after pairing are shown above the plot. Reversing the pairing protocol (-10 ms, right) triggered long-term depression in a different cell. **(b)** Summary plot of changes in EPSP slope following +10 and -10-ms pairing protocols. Neither pairing protocol affected input resistance (R_{in} bottom). **(c)** Summary of changes in EPSP slope versus pairing interval (Δt). * $P < 0.02$, ** $P < 0.005$. **(d)** Two-photon image of a granule cell with a stimulating electrode (Stim) in the external plexiform layer. **(e)** Plot of normalized EPSP slope following +10-ms pairing of distal stimuli with postsynaptic action potentials in four cells. Inset, average response before and 20 min after pairing. Data are presented as mean \pm s.e.m. Animal procedures were approved by the Case Western Reserve University Institutional Animal Care and Use Committee.

cells for at least 20 min (**Fig. 2e**). IPSPs were evoked at long onset latencies (13.2 ms) relative to the group mean (4.1 ± 1.2 ms; $n = 9$) in the one mitral cell in which TBS failed to potentiate inhibitory responses. The increase in IPSP amplitude was statistically significant across the population of eight mitral cells with IPSP onset latencies ≤ 6 ms (-1.06 ± 0.20 control versus -1.62 ± 0.31 mV measured from 5–15 min after TBS, $P < 0.02$, paired t test). On average, IPSPs increased to $154 \pm 15\%$ of control amplitudes; this increase was relatively constant over a 20-min recording period after TBS (**Fig. 2f**). In 6 of these 8 mitral cells, the increase in IPSP peak amplitude was statistically significant when tested individually ($P < 0.05$, unpaired t test). Membrane potential was not significantly dif-

ferent before and after TBS (-49.8 ± 0.5 in control versus -49.5 ± 0.4 mV after TBS, $P > 0.05$, $n = 8$).
 These results suggest that proximal excitatory synapses may detect coincident activity in back-projecting piriform cortical cells and postsynaptic granule cell spiking. Long-term plasticity at this synapse was readily induced by pre- and postsynaptic pairings repeated at 20 Hz, which is in the beta/gamma frequency band that is commonly recorded in piriform cortex *in vivo*^{10,11} and enhanced during odor stimulation¹². Plasticity at these synapses is likely to modulate lateral inhibition onto mitral and tufted cells. We found that the same TBS protocol that reliably triggered LTP of excitatory inputs onto granule cells also evoked a long-lasting enhancement of inhibition onto mitral cells. Although potentiation of proximal excitatory drive to granule cells provides an attractive explanation for TBS-mediated enhancement of mitral cell inhibition, other mechanisms may also be involved, including plasticity in the granule cell-to-mitral cell synapse. Much of the lateral and self-inhibition of principal cells in the olfactory bulb is mediated through reciprocal dendrodendritic synapses that are tonically attenuated by extracellular Mg^{2+} , which blocks currents through the NMDA receptors that govern GABA release^{13,14}. In addition to facilitating cortically evoked disinaptic inhibition onto mitral cells, LTP of excitatory inputs to granule cells may also function to enhance dendrodendritic

spikes more reliably following the second than the first shock with paired stimulation. We found that TBS reliably facilitated responses to GCL stimulation (0.26 ± 0.09 evoked action currents before TBS versus 0.50 ± 0.12 from 5–10 min after TBS, $P < 0.05$, paired t test, $n = 9$; **Fig. 2b**). The ability of TBS to facilitate spiking under cell-attached conditions suggests that synaptic potentiation also can be recorded intracellularly, near the resting potential of granule cells (-67 mV in this study). We tested this in six current-clamp recordings from granule cells held at -70 mV. In 1 of 6 granule cells tested, TBS converted subthreshold test EPSP responses to suprathreshold discharges that precluded measuring EPSP slope reliably. EPSP slope increased in all five cells whose responses remained subthreshold to $122 \pm 4.9\%$ of control (significantly different from control, $P < 0.02$; example in **Supplementary Fig. 5** online). We also found that TBS effectively potentiated EPSPs in granule cells recorded at -70 mV in slices from late juvenile rats (postnatal day 30 rat; **Supplementary Fig. 6** online).

Finally, we asked whether TBS also potentiated inhibition onto mitral cells. We analyzed responses from nine mitral cells that showed clear inhibitory responses to single GCL shocks (**Fig. 2c**). IPSPs evoked by GCL stimulation appeared to be mediated predominately by GABA_A receptors, as they reversed polarity near -70 mV and were blocked by gabazine (10 μ M; **Fig. 2d**). TBS potentiated IPSPs in 8 out of 9 mitral

different before and after TBS (-49.8 ± 0.5 in control versus -49.5 ± 0.4 mV after TBS, $P > 0.05$, $n = 8$).

These results suggest that proximal excitatory synapses may detect coincident activity in back-projecting piriform cortical cells and postsynaptic granule cell spiking. Long-term plasticity at this synapse was readily induced by pre- and postsynaptic pairings repeated at 20 Hz, which is in the beta/gamma frequency band that is commonly recorded in piriform cortex *in vivo*^{10,11} and enhanced during odor stimulation¹². Plasticity at these synapses is likely to modulate lateral inhibition onto mitral and tufted cells. We found that the same TBS protocol that reliably triggered LTP of excitatory inputs onto granule cells also evoked a long-lasting enhancement of inhibition onto mitral cells. Although potentiation of proximal excitatory drive to granule cells provides an attractive explanation for TBS-mediated enhancement of mitral cell inhibition, other mechanisms may also be involved, including plasticity in the granule cell-to-mitral cell synapse. Much of the lateral and self-inhibition of principal cells in the olfactory bulb is mediated through reciprocal dendrodendritic synapses that are tonically attenuated by extracellular Mg^{2+} , which blocks currents through the NMDA receptors that govern GABA release^{13,14}. In addition to facilitating cortically evoked disinaptic inhibition onto mitral cells, LTP of excitatory inputs to granule cells may also function to enhance dendrodendritic

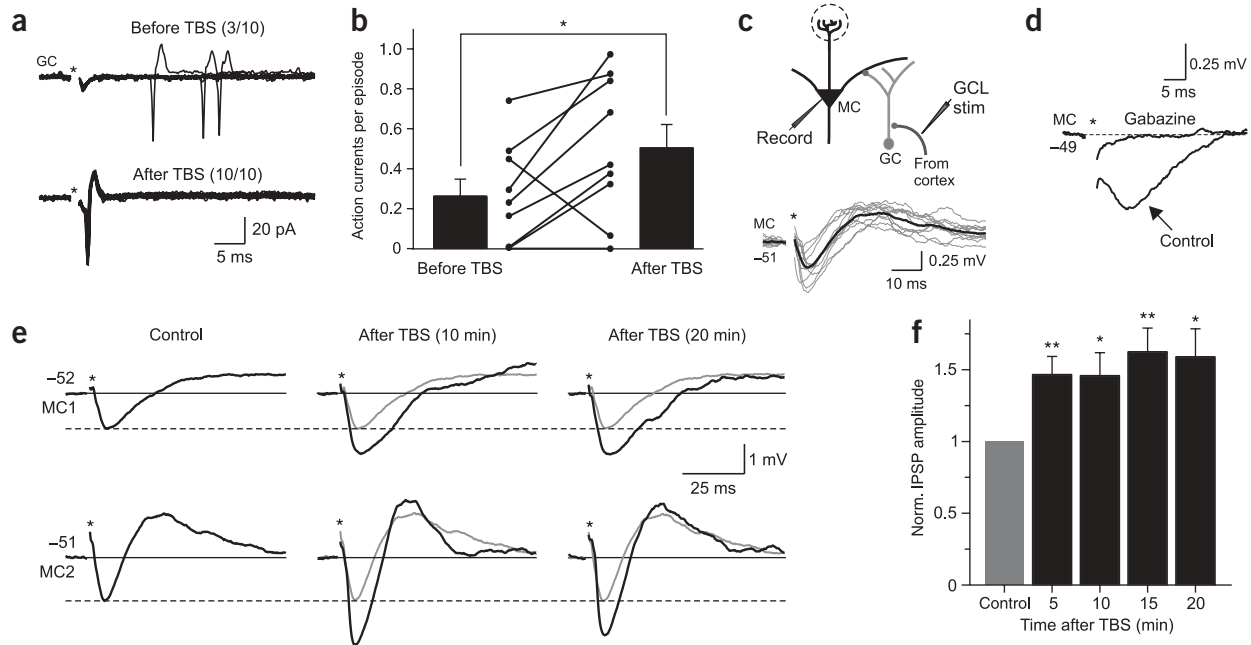


Figure 2 LTP evoked by TBS. (a) Superimposed responses to ten GCL stimuli before and 5 min after TBS. The fraction of episodes with evoked action currents within 50 ms of the stimulus is indicated above each panel. GC, granule cell. (b) Summary of the effect of TBS in nine cell-attached granule cell recordings. Data points indicate the mean number of action currents per episode with latencies < 50 ms after the test stimulus ($n = 30$ control and 30 episodes, 5–10 min after TBS for each cell). TBS increased the effectiveness of test stimuli evoking action currents in 7 out of 9 cells. The mean number of action currents per episode evoked by test stimuli increased significantly following TBS (filled bars, $* P < 0.05$). (c) Top, schematic diagram illustrating an intracellular recording from a mitral cell (MC) and extracellular stimulation in the GCL. Bottom, IPSPs evoked by GCL stimulation recorded in a mitral cell held at -51 mV. Superimposed single trials (gray traces) and the average of ten consecutive responses are shown. (d) Blockade of GCL-evoked IPSP in a mitral cell by $10 \mu\text{M}$ gabazine. (e) TBS potentiated mitral cell inhibition. The responses that are shown are averages of ten trials for each time point from two different mitral cells. Control responses (gray) are superimposed on responses 10 and 20 min after TBS (bold traces). Dashed lines indicate peak amplitude of control responses. (f) Summary of changes in normalized IPSP amplitude after TBS ($n = 8$). Responses were averaged over 30 trials for each time point in each mitral cell. Data are presented as mean \pm s.e.m. $** P < 0.01$.

inhibition indirectly by increasing granule cell spiking, thereby transiently relieving the Mg^{2+} blockade of NMDA receptors at dendrodendritic synapses. Previous studies have demonstrated that extracellular tetanic stimulation in the GCL¹⁵ or activation of piriform cortical cells⁸ can gate dendrodendritic self-inhibition of mitral cells, perhaps via this mechanism. LTP of proximal inputs to granule cells may function to facilitate spiking in specific subpopulations of granule cells, dynamically regulating lateral inhibition onto synaptically coupled mitral cells.

Note: Supplementary information is available on the Nature Neuroscience website.

ACKNOWLEDGMENTS

We thank T. Pressler and P. Larimer for helpful discussions and constructive comments on this manuscript. This work was supported by US National Institutes of Health grant R01-DC04285 to B.W.S.

AUTHOR CONTRIBUTIONS

Y.G. and B.W.S. designed the experiments, analyzed the data and wrote the manuscript. Y.G. conducted the experiments.

Published online at <http://www.nature.com/natureneuroscience/>
Reprints and permissions information is available online at <http://npg.nature.com/reprintsandpermissions/>

1. Bruce, H.M. *Nature* **184**, 105 (1959).
2. Brennan, P.A. & Keiverne, E.B. *Prog. Neurobiol.* **51**, 457–481 (1997).
3. Lévy, F. *et al. Behav. Neurosci.* **104**, 464–469 (1990).
4. Kendrick, K.M., Lévy, F. & Keiverne, E.B. *Science* **256**, 833–836 (1992).
5. Wilson, D.A., Sullivan, R.M. & Leon, M. *Brain Res.* **354**, 314–317 (1985).
6. Satou, M., Anzai, S. & Huruno, M. *J. Comp. Physiol. A Neuroethol. Sens. Neural. Behav. Physiol.* **191**, 421–434 (2005).
7. Haberly, L.B. & Price, J.L. *J. Comp. Neurol.* **178**, 711–740 (1978).
8. Balu, R., Pressler, R.T. & Strowbridge, B.W. *J. Neurosci.* **27**, 5621–5632 (2007).
9. Sjöström, P.J. & Häusser, M. *Neuron* **51**, 227–238 (2006).
10. Zibrowski, E.M. & Vanderwolf, C.H. *Brain Res.* **766**, 39–49 (1997).
11. Neville, K.R. & Haberly, L.B. *J. Neurophysiol.* **90**, 3921–3930 (2003).
12. Ravel, N. *et al. Eur. J. Neurosci.* **17**, 350–358 (2003).
13. Isaacson, J.S. & Strowbridge, B.W. *Neuron* **20**, 749–761 (1998).
14. Schoppa, N.E. *et al. J. Neurosci.* **18**, 6790–6802 (1998).
15. Halabisky, B. & Strowbridge, B.W. *J. Neurophysiol.* **90**, 644–654 (2003).